Electronic Supplementary Information

Direct Visualization of Initial SEI Morphology and Growth Kinetics During Lithium Deposition with *in situ* Electrochemical Transmission Electron Microscopy

Robert L. Sacci,[a] Nancy J. Dudney, [a] Karren L. More, [b] Lucas R. Parent, [c] Ilke Arslan, [c] Nigel D. Browning, [c] and Raymond R. Unocic [b]

[a] Materials Science and Technology Division, Oak Ridge National Laboratory, Oak Ridge, TN 37831, USA.
[b] Center for Nanophase Materials Sciences, Oak Ridge National Laboratory, Oak Ridge, TN 37831, USA.
[c] Fundamental & Computational Sciences Directorate, Pacific Northwest National Laboratory, Richland, WA 99352, USA.

Corresponding Authors:
saccirl@ornl.gov
unocicrr@ornl.gov

Movie S1. *In situ* observations of dendrite nucleation and growth from the corner of the gold working electrode during a cyclic voltammetry experiment at 20 mV/s in a 1.2M $LiPF_6$ EC:DMC electrolyte.

Materials and Experimental Procedure

For this study, a liquid flow cell *in situ* TEM holder with electrical biasing capabilities was used (Hummingbird Scientific, Lacey, WA). This system incorporates two silicon microchip devices that fit inside the tip of the TEM holder. Each microchip contains a 50 x 200 μm electron transparent silicon nitride-viewing region. The lower spacer microchip has two parallel areas of 500 nm thick SU-8, which serve the purpose of creating a channel through which electrolyte is delivered to the electrochemical cell. The upper electrochemical microchip has three gold electrodes that have been microfabricated on the surface of the SiN_x membrane. To clean the microchips prior to use, they were rinsed in acetone then methanol. After the microchips dried, plasma cleaning was done for cleaning residual organic residue and to render the surface of the SiN_x membranes hydrophilic. Due to the high vapour pressure and air/moisture sensitivity of the 1.2M $LiPF_6$ EC:DMC electrolyte (Novolyte Technologies), assembly of the electrochemical cell into the *in situ* TEM holder was performed in an argon filled glovebox. With the SiN_x membranes face-to-face, the spacer microchip and electrochemical microchips were placed in the *in situ* TEM holder. The SiN_x membrane viewing windows were aligned with the aide of a stereomicroscope inside the glovebox. The microchips were then sealed with o-rings and a cover plate. The battery grade electrolyte was then introduced through the holder and in between the microchips with a microfluidic syringe pump and microfluidic PEEK tubing. Prior to placing the holder into the microscope, the system was placed intro a dry pump station for a leak check.

In situ TEM Experiments

The *in situ* TEM experiments were conducted in a Hitachi HF3300 S/TEM instrument that was operated at 300 kV. The *in situ* TEM holder was connected to a Bio-logic SP-200 potentiostat. The gold electrodes that were microfabricated on the electrochemical microchips were interfaced with the potentiostat such that the center electrode was set at the working electrode and the outer electrodes were set as the counter and reference electrode. For the data presented in this study, a cyclic voltammetry was used at scan rate of 20 mV/s while imaging the gold working electrode at a frame rate of 2 frames-per-second using a Gatan UltraScan CCD camera. Due to the size scale of the gold electrodes, only a small portion of the working electrode can be visualized even at low magnification. The electron beam current (5.8 nA) was directly measured with a Keithly picoammeter and Gatan model 646 TEM holder that is equipped with an

integrated Faraday cup. Under these imaging conditions, we did not observe electrolyte decomposition by the electron beam. The *in situ* video sequences are time-stamped and correlated with the CV data.

Electrochemical Measurements

A three-electrode setup was used for controlling and measuring the potential at the working electrode using a Au-patterned pseudoreference electrode. While the open circuit potential of Au against Li metal in battery electrolyte is typically 2.8 V vs Li/Li^+. All electrodes were briefly polarized to test for electrolyte filling the microfluidic channel. This polarization decreased the OCP of Au to 1.75 V vs Li/Li^+. This is a typical response for electrodes that either intercalate Li or alloy readily with Li. The potential waveform used in this study is shown in Figure S1. Starting at 0 V the potential was swept down to -4 V (-2.25 V vs Li/Li^+) and held there for 3.5 min. The potential was then swept upward to +1 V and held for 4 min.

Maintaining a stable pseudoreference within 100 μm of the working is difficult given the sensitive of pseudoreferences to their environment. That is, chemistries taking place at the working electrode can affect the pseudoreference, which affects the control and measurement of the potential. At the onset of SEI dendrite formation the current shows some spikes due to noise, from probably displacement of tiny bubbles along the reference/counter electrodes. Our setup proved to be stable until high overpotentials were applied (<-2 V). Figure S2 shows an extended view of the recorded CV, which highlights the cell instability during bulk Li deposition. Here the *IR*-dop is significant because the current is relatively high and Li dendrites are expected to form. SEI also forms and changes the local concentration of the $LiPF_6$ and EC. This likely affects the pseudoreference that is 20 μm away. Also problematic to this high current is the high rate of oxidation that must occur at the counter. It was found that the counter electrode is polarized to +6 V during this region, which is well outside the potential region range. Also, the chromium (Cr) adhesion layer underlayer dissolves in this region. We ran 3 cycles with the TEM focused on each electrode to make sure that, the CE/WE were reversible and that the reference electrode was unchanged during cycling. The RE was in fact unchanged, and the CE cycled as expected (Cr dissolution/adsorption), and the WE cycled showing dendrites, SEI/Metallic Li, SEI, Dendrites, SEI/Metallic Li, etc.

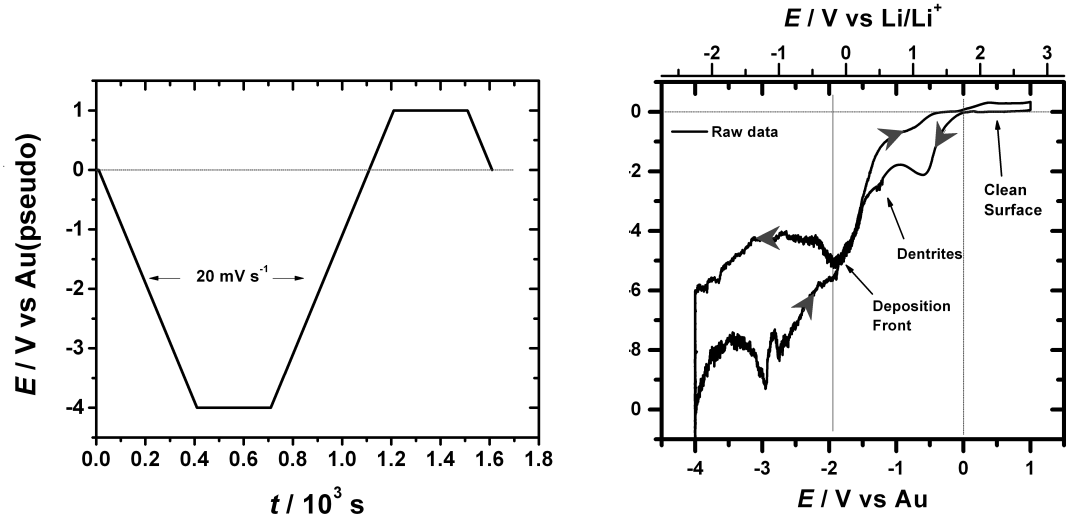

Fig. S1 A) Potential waveform used in this study. B) Full range cyclic voltammogram using waveform depicted in Fig S1A. Line at -2 V marks lost of cell control either due to large *IR*-drop, counter electrode dissolution, or deposition affecting the pseudoreference.

Image Analysis

Due to the low contrast of the dendrites that were observed in the *in situ* experiments, it was necessary to adjust the intensity level, brightness, and contrast in order to enhance the appearance such that quantitative measurements can be obtained. Fig. S2 shows two sets of bright-field TEM images that were extracted from Movie S1. Fig. S2 A-B are shown in black and white images while Fig. S2 C-D are shown in false colored images. The only image processing that was done for these sets of images were adjustment of the intensity level, brightness, and contrast and they were all done consistently so there would be no difference when comparing the images for quantitative analysis of dendrite growth. False coloring of the images are shown in Fig. 3 and Fig. 4 in the manuscript, as well as Fig. S2 C-D, were modified by applying a red/green look-up table using Image J. The red rim around the edge of the Au working electrode is due to the change in electrode thickness, which has a concomitant effect on the bright field TEM image intensity and hence the false coloring.

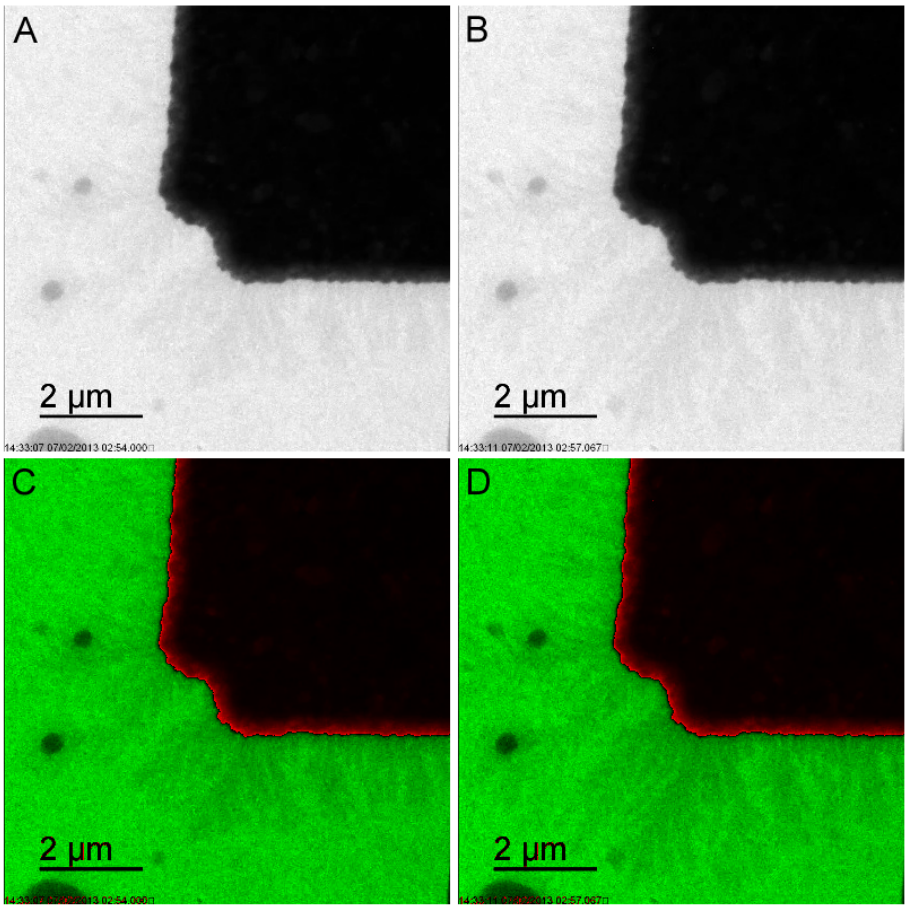

Fig. S2 Comparison between grey-scaled (A-B) and false color (C-D) bright field TEM images. The images were modified by adjusting the intensity level, brightness, and contrast to enhance to appearance of the dendrites. False coloring of the grey-scaled imaged was performed by applying a red/green look-up table.

Quantitative Image Analysis of Dendrite Growth Measurements

Primary dendrite growth measurements were obtained by quantitative image analysis. Here four dendrites were tracked as they nucleated and grow from the Au working electrode. The dendrites are labeled D1-D4 as marked in Fig. 3D in the manuscript. Measurements were obtained by measuring the dendrite tip displacement from sequential BF-TEM images that were extracted from Movie S1. A limited number of measurements were acquired because the dendrites grew past the field of view during in situ video acquisition. The measurement data presented in Fig. S3 shows tip displacement and dendrite velocity as a function of time. Inset labels marked A, B, and C correspond to Fig. 3A-C.

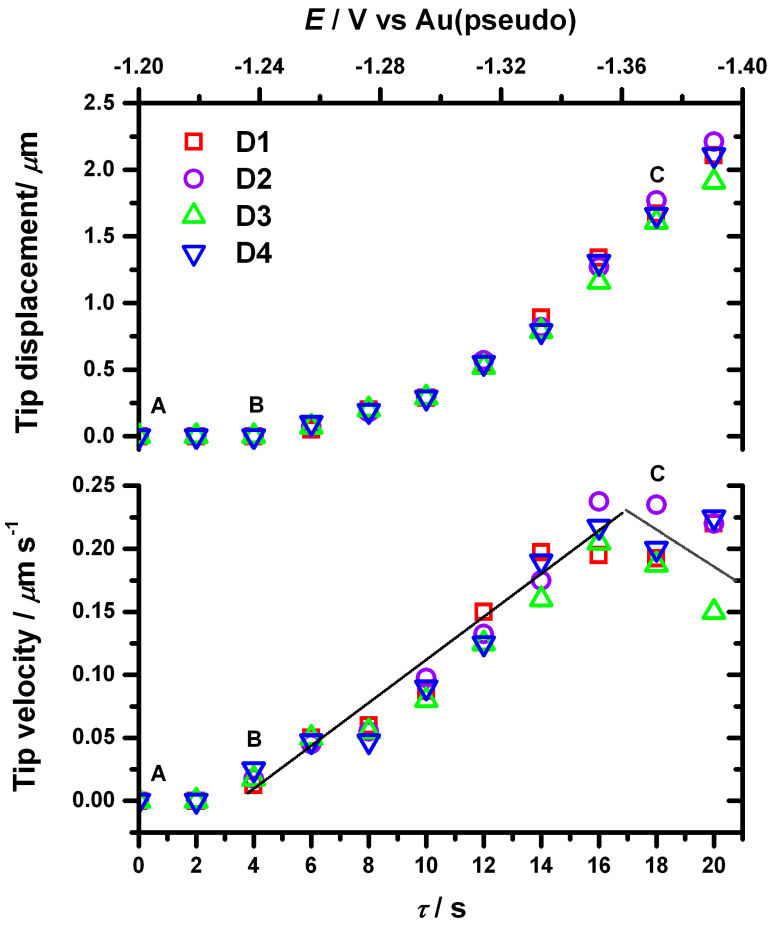

Fig. S3 Plot of primary dendrite tip displacement (upper figure) and primary dendrite tip velocity as a function of time. Data obtained from dendrites observed in Movie S1.